Title

Canted stripe phase evolution due to a spin reorientation transition in Fe films grown on Ag(001) vicinal surface

Journal

Physical Review B, 93(6)

ISSN

2469-9950

Authors

Dąbrowski, M
Cinal, M
Przybylski, M
et al.

Publication Date

2016-02-01

DOI

10.1103/physrevb.93.064414

Peer reviewed

Canted stripe phase evolution due to a spin reorientation transition in Fe films grown on Ag(001) vicinal surface

M. Dąbrowski,[1,*] M. Cinal,[2] M. Przybylski,[1,3] G. Chen,[4] A. T. N'Diaye,[4] A. K. Schmid,[4] and J. Kirschner[1,5]

[1]*Max Planck Institut für Mikrostrukturphysik, 06120 Halle, Germany*

[2]*Institute of Physical Chemistry of the Polish Academy of Sciences, 01-224 Warsaw, Poland*

[3]*Faculty of Physics and Applied Computer Science, and Academic Centre for Materials and Nanotechnology, AGH University of Science and Technology, 30-059 Kraków, Poland*

[4]*NCEM, Lawrence Berkeley National Laboratory, Berkeley, California 94720, USA*

[5]*Naturwissenschaftliche Fakultät II, Martin Luther Universität Halle-Wittenberg, 06120 Halle, Germany*

(Received 24 December 2015; revised manuscript received 26 January 2016; published 10 February 2016)

The evolution of the domain structure with the thickness of bcc Fe films deposited on the Ag(116) vicinal surface is studied by spin-polarized low-energy electron microscopy. We show that a spin reorientation transition proceeds via two mechanisms: continuous rotation of magnetization within the vertical plane perpendicular to the steps and discontinuous reorientation of the in-plane component of magnetization, leading to splitting of the domains. In contrast to previously investigated systems with stripe domains, we reveal that in the case of a vicinal ferromagnetic surface, the domain width increases while changing the orientation of the magnetization from a canted out-of-plane state into an in-plane state. A theoretical model developed in this work successfully describes the domain structure behavior observed in our experiments and can be equally applied to other ferromagnetic films grown on vicinal surfaces.

DOI: 10.1103/PhysRevB.93.064414

I. INTRODUCTION

One of the key features of ferromagnetic films with the easy axis of the magnetization oriented perpendicular to the sample plane is the formation of a stripe domain phase. The stripe phase is the result of the competition between the exchange interaction, favoring parallel alignment of spins, and dipolar interaction, which favors antiparallel alignment over large distances [1–3]. Considerable attention has been paid to studies of stripe domains in the vicinity of a spin reorientation transition (SRT), where a rapid decrease of the domains' size upon increasing the film thickness has been observed in Fe/Cu(001) [4,5] and Co/Au(111) [6–8]. These pronounced variations of the domain size are in very good agreement with theoretical predictions [2] and are associated with a decrease of the effective anisotropy energy $K_{\mathrm{eff}} = K_s - K_{\mathrm{dip}}$ (since the dipolar anisotropy K_{dip} increases, while the perpendicular magnetocrystalline anisotropy K_s remains roughly constant, upon increasing the film thickness).

The fundamental question is whether the above scenario remains valid for all ferromagnetic thin films with perpendicular magnetization. In particular, how the SRT proceeds in systems with reduced symmetry, like films grown on stepped/vicinal surfaces. For films grown on vicinal surfaces the competition between magnetocrystalline anisotropy terms, preferring orientations of magnetization **M** along the principal crystallographic directions, and the dipolar anisotropy, preferring an orientation of **M** in the film plane (which, for vicinal surfaces is not equivalent to the principal crystallographic planes) [9], results in tilted orientations of **M**. Since the dipolar energy of stripe domain system is postulated to depend on the magnetization direction [10], it makes the description of the magnetic anisotropy more complex because the effective anisotropy constant K_{eff} can depend on the tilting angle. Yet a separate problem is an appropriate definition of such an anisotropy constant for stepped films.

In this article we combine theoretical and experimental studies in order to understand the SRT mechanism in ferromagnetic film on vicinal surfaces. By employing spin-polarized low energy microscopy (SPLEEM) [11], we observe the evolution of the magnetic microstructure as a function of thickness of Fe film grown on the Ag(116) vicinal surface. The well-known surface preparation and properties [12–16] make Fe/Ag(116) well suited for studies of the SRT process on the microscopic level. We show that the SRT from out-of-plane to in-plane orientation consists of two stages: (i) continuous rotation of magnetization direction within stripe domains and (ii) discontinuous switching of the in-plane component of the magnetization. We also demonstrate that domain size increases exponentially with increasing the film thickness. Our experimental results are explained within a theoretical model. The domain size and the magnetization orientation obtained from the experiment allow us to determine the dependence of the anisotropy constants on the film thickness.

The outline of the paper is as follows. In Sec. II we present a theoretical model that allows us to calculate the domain size and the effective anisotropy constant for films with arbitrary magnetization direction and reduced symmetry due to their deposition on a vicinal substrate. Section III is devoted to experimental details. A discussion and analysis of the experimental results within the framework of our model is carried out in Sec. IV. Finally, the main conclusions are summarized in Sec. V.

II. THEORY

The magnetostatic energy E_{dip} for a system of stripe magnetic domains with sharp domain walls in a ferromagnetic

*Corresponding author: mdabrows@pitt.edu; Present address: Department of Physics and Astronomy, University of Pittsburgh, Pittsburgh, PA 15260, USA.

film has previously been calculated within the continuum approximation for magnetization **M** perpendicular to the film surface. The expression of $E_{\rm dip}$ per unit volume obtained by Kooy and Enz [17],

$$E_{\rm dip}(t,D) = \frac{16M_{\rm s}^2}{\pi^2}\frac{D}{t}\sum_{\substack{n=1\\(n\ \rm odd)}}\frac{1}{n^3}[1-e^{-n\pi t/D}], \qquad (1)$$

depends on the domain size D, the film thickness t, and the saturation magnetization $M_{\rm s}$. Based on the expression (1), Kaplan and Gehring [2] derived the following formula for the optimum domain size:

$$D = 0.954\, t e^{\pi D_0/(2t)}\ . \qquad (2)$$

The characteristic length $D_0 = \sigma_{\rm w}/(2\pi M_{\rm s}^2)$ is defined with the domain wall (DW) energy $\sigma_{\rm w}$ (per unit area of the wall) and the density $2\pi M_{\rm s}^2$ of the magnetostatic energy in a ferromagnetic film in the monodomain state (i.e., for $D\to\infty$) with magnetization perpendicular to the film surface. The formula is valid for $t \ll D_0$.

A. Dipolar anisotropy energy for arbitrary magnetization direction

We expand the expression for the magnetostatic energy $E_{\rm dip}$ to arbitrary orientation of magnetization **M**, described by the polar angle θ with respect to the film surface normal and the azimuthal angle φ with respect to the atomic steps (as shown schematically in Fig. 2). For convenience we introduce the azimuthal angle of the magnetization with respect to the DW planes $\widetilde{\varphi} = \varphi - \varphi_{\rm DW}$, where $\varphi_{\rm DW}$ denotes the orientation of the DWs with respect to the steps. The following formula,

$$E_{\rm dip}(t,D,\theta,\widetilde{\varphi}) = E_{\rm dip}(t,D;\theta=0)(\cos^2\theta - \sin^2\theta\sin^2\widetilde{\varphi}) + 2\pi M_{\rm s}^2\sin^2\theta\sin^2\widetilde{\varphi}, \qquad (3)$$

is derived by representing $E_{\rm dip}$ with the scalar magnetic potential and subsequent use of the Poisson equation; the concise derivation is given in the Appendix.

B. Domain size for arbitrary magnetization direction

According to Eq. (3), the dependence of $E_{\rm dip}(t,D,\theta,\widetilde{\varphi})$ on the film thickness t and the domain size D is determined by the term including $E_{\rm dip}(t,D;\theta=0)$, given by the expression (1). Thus, the part of $E_{\rm dip}(t,D,\theta,\widetilde{\varphi})$ dependent on t and D is immediately found with Eq. (1), if the constant $2\pi M_{\rm s}^2$ is replaced with the angle-dependent factor $2\pi M_{\rm s}^2(\cos^2\theta - \sin^2\theta\sin^2\widetilde{\varphi})$. In consequence, the optimum domain size D, found by minimizing the total energy density $E_{\rm dip}(t,D,\theta,\widetilde{\varphi}) + \sigma_{\rm w}/D$ with respect to D, is also given by formula (2) provided that the expression for the characteristic dipolar length D_0 is modified as follows:

$$D_0(\theta,\widetilde{\varphi}) = \frac{\sigma_{\rm w}}{2\pi M_{\rm s}^2(\cos^2\theta - \sin^2\theta\sin^2\widetilde{\varphi})}\ . \qquad (4)$$

In the particular case when the magnetization **M** is parallel to DWs ($\varphi = \varphi_{\rm DW}$), the dipolar length is given by

$$D_0(\theta,\widetilde{\varphi}=0) = \frac{\sigma_{\rm w}}{2\pi M_{\rm s}^2\cos^2\theta}\ . \qquad (5)$$

This formula was recently assumed in Ref. [10], based on the interpretation of Eq. (2) that D_0 is given by the ratio of $\sigma_{\rm w}$ and the magnetostatic energy of the monodomain film $2\pi M_{\rm s}^2\cos^2\theta$, not only for the magnetization perpendicular to the film surface ($\theta = 0$), but also for a tilted magnetization. The formula (5) is presently shown to be valid, but only for $\widetilde{\varphi} = 0$, as it seen in Eq. (4).

It is clearly seen from the relations (2) and (5) that the domain size D increases with increasing tilting angle θ for fixed t and $\sigma_{\rm w}$. The domain size D depends on the film thickness t through both the explicit occurrence of t in Eq. (2) as well as due to the thickness dependencies of θ and the effective anisotropy constant $K_{\rm eff}$, which affects the DW energy $\sigma_{\rm w}$.

C. Effective anisotropy within the plane perpendicular to the steps

The domain wall energy

$$\sigma_{\rm w} = 4\sqrt{AK_{\rm eff}} \qquad (6)$$

depends in a simple way on the effective anisotropy constant $K_{\rm eff}$ (per unit volume) and the exchange stiffness constant A. This expression is valid for a 180° DW of the Bloch type where the angular dependence of energy $-K_{\rm eff}\cos^2(\theta-\theta_0)$ on the magnetization rotating within the wall is defined with the uniaxial anisotropy $K_{\rm eff}$ and the angle θ_0 that corresponds to the easy axis (with the assumption that $\varphi = \varphi_{\rm DW}$). Such dependence is in fact also valid for thin stepped films with magnetization tilted from the surface normal within the plane perpendicular to the steps, if the bulk anisotropy, which is of the fourth order in spin-orbit coupling, is negligible in comparison with the second-order anisotropy terms arising from the reduced symmetry of a stepped film.

The energy of a monodomain ferromagnetic film on a stepped substrate depends on the direction of the magnetization **M** as follows [13]:

$$\begin{aligned} E(\theta,\varphi) &= K_{\rm dip}\cos^2\theta + K_{\rm s}\sin^2\theta' - K_{\rm u}\sin^2\theta'\cos^2\varphi' \\ &\quad - \tfrac{1}{2}K_{\rm sp}\sin 2\theta'\sin\varphi' + E_{\rm bulk}(\theta',\varphi') \\ &\equiv K_{\rm dip}\cos^2\theta + E^{(2)} + E_{\rm bulk} \\ &\equiv K_{\rm dip}\cos^2\theta + E_{\rm MCA}(\theta',\varphi'), \end{aligned} \qquad (7)$$

where θ' and φ' denote angles measured with respect to the Ag crystallographic axes [001] (normal to the terraces surface) and [$\bar{1}$10] (in the terraces plane, parallel to the steps), respectively. The expression (7) includes the usual form of the shape anisotropy energy (i.e., the magnetostatic energy of the ferromagnetic film in the monodomain state). The shape anisotropy constant is equal to $K_{\rm dip} = 2\pi M_{\rm s}^2 t$ if the system energy E is calculated per unit area of the film surface. The magnetocrystalline energy $E_{\rm MCA}$ arising from the spin-orbit interaction (treated as a perturbation in the Hamiltonian) comprises the second-order energy correction $E^{(2)}$ and the fourth-order contribution $E_{\rm bulk}$ corresponding to bulk anisotropy. The second-order contribution is expressed with the three anisotropy constants $K_{\rm s}$, $K_{\rm sp}$, and $K_{\rm u}$, where the latter two arise due to reduced symmetry in films on a vicinal substrate.

If the magnetization **M** is perpendicular to the steps (i.e., $\varphi = \varphi' = 90^\circ$), we have

$$\theta = \theta' + \alpha, \tag{8}$$

where α denotes the vicinal angle. If the bulk anisotropy is neglected, the film energy (7) can then be written as

$$\begin{aligned} E_\perp(\theta) &= E(\theta,\varphi = 90^\circ) = -K_{\text{eff}}\cos^2(\theta' - \theta'_0) + \text{const} \\ &= -K_{\text{eff}}\cos^2(\theta - \theta_0) + \text{const}, \end{aligned} \tag{9}$$

where the following trigonometric identities $\cos 2\gamma = 2\cos^2\gamma - 1$ (for $\gamma = \theta, \theta', \theta' - \theta'_0$) and $\cos(2\theta' - 2\theta'_0) = \cos 2\theta \cos 2\theta_0 + \sin 2\theta \sin 2\theta_0$ have been applied. The effective anisotropy constant is defined as

$$K_{\text{eff}} = \sqrt{(K_{\text{dip}}\cos 2\alpha - K_{\text{s}})^2 + (K_{\text{dip}}\sin 2\alpha - K_{\text{sp}})^2}, \tag{10}$$

with the three anisotropy constants K_{dip}, K_{s}, K_{sp} and the vicinal angle α. The expression for $E_\perp(\theta)$ is valid in the extended angle range $0^\circ \leqslant \theta \leqslant 360^\circ$, which describes all possible orientations of the magnetization within the plane perpendicular to the steps. In such description the angle interval $180^\circ < \theta \leqslant 360^\circ$ corresponds to the polar angle $(360^\circ - \theta) < 180^\circ$ and the azimuthal angle $\varphi = -90^\circ$ in the standard definition of these angles.

The tilting angle $\theta_0 = \theta'_0 + \alpha$ corresponds to the easy axis and it can be found from the relation

$$\tan 2\theta'_0 = \frac{K_{\text{dip}}\sin 2\alpha - K_{\text{sp}}}{K_{\text{dip}}\cos 2\alpha - K_{\text{s}}}, \tag{11}$$

which is obtained from the energy extremum condition $\partial E_\perp/\partial\theta' = 0$ applied to $E_\perp(\theta') = E(\theta = \theta' + \alpha, \varphi = 90^\circ)$ found from Eq. (7). The choice between θ'_0 and $\theta'_0 + 90^\circ$, which both satisfy Eq. (11), is done based on the energy minimum auxiliary condition $\partial^2 E_\perp/\partial\theta'^2 > 0$. Thus we are left with two values of the tilting angle θ'_0 ($<180^\circ$) and $\theta'_0 + 180^\circ$, corresponding to the opposite directions of the magnetization, which are equivalent in the absence of external fields.

III. EXPERIMENTAL DETAILS

The experiments were performed in an ultrahigh-vacuum system with a base pressure of 2×10^{-11} Torr. An Ag(116) vicinal crystal [13.3° off the (001) surface] with the step edges oriented along the $[\bar{1}10]$ direction was used. The Ag(116) surface was cleaned by cycles of Ar ion sputtering at 1 keV and annealing at ~775 K. Scanning tunneling microscopy (STM) images (not shown) confirm that this preparation procedure yields vicinal surfaces characterized by regular monoatomic steps with an average terrace width of 0.86 nm. These regular step arrays also cause sharp double-split diffraction spots in low-energy electron diffraction (LEED), and in the work reported here we used LEED imaging to confirm surface quality prior to SPLEEM experiments. Fe films were grown *in situ* and at room temperature in the SPLEEM instrument. During deposition, low-energy electron reflectivity oscillations associated with layer-by-layer film growth were used for precise growth rate and film thickness measurements. (This approach was described previously, for example in Ref. [5].) In order to explore detailed magnetic properties at high thickness resolution, for this work wedge-shaped films of 1 mm width and ~14 monolayer (ML)/mm slope were prepared by placing a shutter into the Fe molecular beam. After growth, the films were warmed up to 450 K in order to improve the surface morphology [12].

The domain structure of Fe/Ag(116) was imaged by using spin-polarized low energy microscopy [18,19]. The magnetic contrast in SPLEEM is quantified by the asymmetry intensity $A_{ex} = (1/P)(I_\uparrow - I_\downarrow)/(I_\uparrow + I_\downarrow)$, where $I_\uparrow$ and $I_\downarrow$ represent the reflected intensities for antiparallel polarized incident electron beams and P denotes the degree of incident electron beam polarization (~20% in this case). Subtraction of $I_\uparrow$ and $I_\downarrow$ and subsequent division by their sum eliminates the nonmagnetic features of the image and yields an asymmetry image in which intensities are proportional to the incident beam polarization and the component of the local magnetization vector along the incident beam polarization direction. By measuring the magnetic contrast in three orthogonal polarizations of the incident beam, three components of the magnetization vector, M_x, M_y, and M_z, are derived and the local three-dimensional magnetization vector can be determined. The magnetic contrast in SPLEEM is determined by the spin-dependent band structure and therefore, changes with energy [20]. By taking several SPLEEM images at different electron energies and different Fe thicknesses, we found the optimum contrast at energy $E = 13.5$ eV. The measurements were performed at two temperatures: 300 and 130 K.

In a typical SPLEEM experiment, a spin-polarized low-energy electron beam is directed towards the sample surface at normal incidence, and the specular beam of the backscattered electrons is magnified in an electron-optical column to form an image of the sample surface (bright-field mode) [21,22]. Interestingly, we have found that in the case of our sample, the imaging of the first-order diffraction beam (dark-field mode) [21,22] significantly enhances the magnetic contrast in comparison to the usually used bright-field mode. This is due to the fact that the atomic terraces in our vicinal surface are perpendicular to the [001] direction, which is 13.3° off the sample normal. By tilting the macroscopic plane of the sample by ~2–3°, the incident electron beam impinges the surface at off-normal angle and brings the desired first-order diffraction beam close to the optical axis of the microscope's projection column.

IV. RESULTS

SPLEEM measurements for three orthogonal electron polarizations have been performed in the Fe film thickness range from 0 to 14 ML at 130 and 300 K. Thickness-dependent SPLEEM images were acquired by moving the sample position across the Fe wedge with respect to the microscope's optical axis. The triplets of SPLEEM images for chosen thicknesses of Fe film are shown in Fig. 1. The domain structures at 130 and 300 K are qualitatively similar and the images at 130 K are shown solely. Blue and red regions result from the component of the surface magnetization vector along the axis defined by the orientation of the spin polarization of the illuminating beam (parallel and antiparallel, respectively). No magnetic contrast ($A_{ex} = 0$), i.e., white color in SPLEEM images, is observed

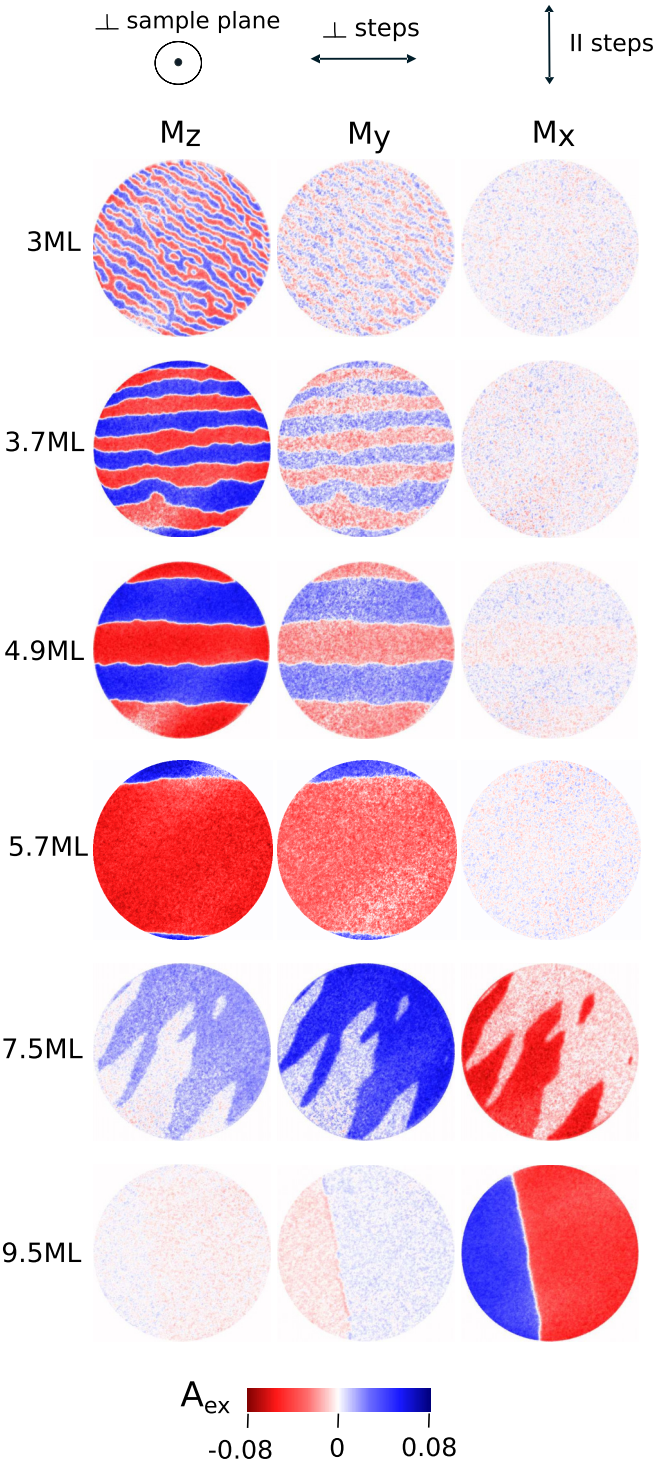

FIG. 1. SPLEEM images with varying thickness of Fe film grown on a Ag(116) surface obtained at 130 K. The color scale represents orientation of magnetization **M** with respect to the polarization **P** of the incident beam. (Blue and red areas correspond to parallel and antiparallel orientations of **M** and **P**, respectively.) The polarization direction of the illuminating beam is indicated on top of the image columns. The images are 11.5 μm in diameter.

for the polarization of the incident beam perpendicular to the direction of magnetization at the surface or if $|\mathbf{M}| = 0$ (nonmagnetic surface).

The lowest thickness of Fe film at which any domain structure was distinguished is 2.85 ML. Since the Curie temperature T_C for 2.5-ML-thick bcc Fe film grown on Ag(001) was reported to be around 325 K [23,24], it is plausible that reduced Curie temperature is responsible for the absence of the magnetic contrast below 2.85 ML.

At film thickness above 2.85 ML, SPLEEM images acquired with the polarization **P** of the incident beam aligned perpendicular to the surface plane show the formation of an out-of-plane stripe domain phase (left column in Fig. 1). As the Fe film thickness increases, stripe domains expand and arrange to an alignment where the DWs are oriented perpendicular to the step edges. Starting at around 4 ML, a continuous increase of the contrast is observed in images acquired with the polarization **P** of the incident beam aligned in-plane and perpendicular to the step edges (middle column in Fig. 1). Up to around 7 ML, only negligible magnetic contrast is observed when the beam polarization is aligned parallel to the step edges (right column in Fig. 1), which means that there is no magnetization component along this direction (M_x nearly zero). For 7.5-ML-thick Fe film, the domain pattern changes dramatically. A rapid change of the magnetization orientation is manifested by a significant reduction of the out-of-plane signal (left panel marked 7.5 ML) accompanied by an increasing in-plane signal (middle and right panels marked 7.5 ML) and splitting of the stripe domains.

In the film thickness range of about 4–7 ML the simultaneous presence of out-of-plane (left column) and in-plane (middle column) magnetic contrast means that the magnetization vector is canted. In contrast to more complex canted magnetization structures observed in films grown on low-index substrates [25,26], the vicinal substrate used in our experiment locks the azimuthal orientation of the canting angle and the magnetization vector rotates within the vertical plane perpendicular to the surface steps.

The substantial out-of-plane magnetic contrast observed in the films of thicknesses up to 7.5 ML (left column, Fig. 1) essentially vanishes in 9.5-ML-thick films, indicating that at this thickness the magnetization is oriented nearly exactly in the sample plane. In addition, the magnetic contrast is visible exclusively in images acquired with beam polarization parallel to the step edges (9.5 ML in Fig. 1), indicating that the SRT into the sample plane is accompanied by an abrupt switching of the in-plane magnetization component into the direction along the step edges. The domains are larger (in comparison to thinner Fe films) and DWs have no preferential orientation with respect to substrate steps. Moreover, DW spin structure can be now observed from the magnetic contrast perpendicular to the easy axis of magnetization (see 9.5-ML-thick Fe film in Fig. 1, middle panel), indicating that Neél-type domain walls are present [27].

This Fe film-thickness-dependent SRT summarized in Fig. 1 can be described more quantitatively by measuring the canting angle θ and azimuthal angle φ for every domain from the amount of magnetic contrast in the SPLEEM images. This measurement is plotted in Fig. 2, where the angles θ and φ are defined with respect to the crystallographic directions of the Ag(116) substrate as shown in the inset. Note that for clarity of this plot we avoided negative angles by rotating domains pointing down by 180°.

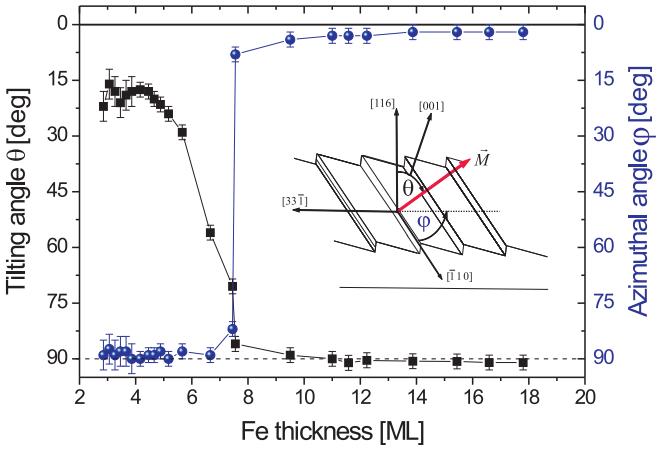

FIG. 2. Tilting angle θ and azimuthal angle φ of magnetization as a function of Fe film thickness evaluated from SPLEEM images obtained at 130 K.

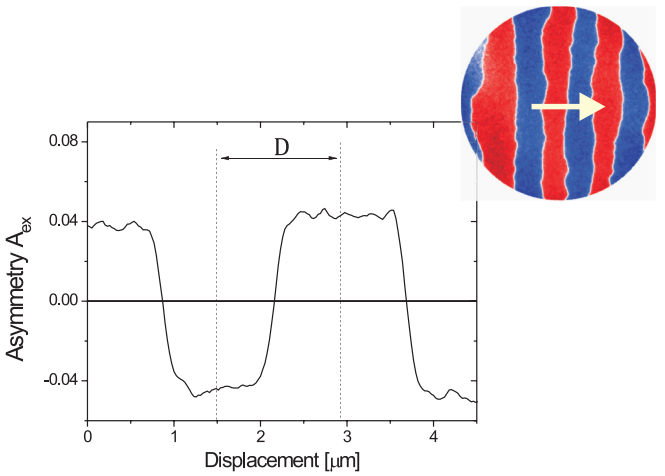

FIG. 3. The line profile along the white arrow in the SPLEEM image (see inset) obtained for a 3.9-ML-thick Fe film with the polarization axis of electrons perpendicular to the sample plane. The domain size (the stripe width) D is defined as the distance between the centers of two neighboring domains.

The orientation of the magnetization as a function of Fe film thickness at 130 K is shown in Fig. 2. Initially, starting from the thinnest investigated Fe film, magnetization is canted away from the sample normal by $\sim 20^\circ$ with the inclination towards the direction perpendicular to the steps ($\varphi = 90^\circ$). This means that **M** is oriented nearly along the [001] direction, i.e., perpendicular to the terrace's plane (the miscut angle between the [001] and [116] directions for Ag(116) crystal is equal to 13.3°). Up to the film thickness of 5 ML there are no significant changes in orientation of the magnetization. Above 5 ML, the tilting angle starts to increase while keeping the azimuthal orientation perpendicular to the steps. At 7.5 ML, an abrupt change of θ and a discontinuous switch of the in-plane magnetization orientation from perpendicular to the steps toward along the steps ($\varphi = 90^\circ \rightarrow \varphi = 0^\circ$) is observed. This rapid change of the orientation of magnetization is associated with the splitting of the stripe domains, as shown in Fig. 1. With further increase of Fe thickness, the orientation of magnetization remains the same, i.e., in-plane along the step edges. The dependence of the tilting angle θ and the azimuthal angle φ on Fe film thickness obtained at 300 K (not shown) is nearly identical as at 130 K.

When well-ordered stripe domains are present, the domain size D can be estimated by taking line profiles across the domain walls (see Fig. 3). We define the domain size D as a distance between the centers of two oppositely oriented domains. The domain size for given Fe thickness is the average value within the field of view (11.5 μm).

The thickness dependence of the domain size D at two different temperatures, 130 and 300 K, is shown in Fig. 4. Starting with the thinnest Fe films, the size of the domains D increases exponentially with the film thickness. At around 4.5 ML, the domains measured at 130 K are over 2 times larger than those measured at 300 K. Interestingly, with further increase of the Fe film thickness, the domains measured at 130 K become similar to those measured at 300 K. Above 5 ML the domain size increases rapidly at both temperatures and eventually exceeds the field of view ($D > 11.5\ \mu$m).

Note that the measurement was performed on a wedge sample and there is a thickness gradient, which is perceptible, even within the area of a single image. (The spread of the thickness within the field of view, from the top to the bottom, is around 0.16 ML.) As a consequence, it can be observed that within the single image, there is a gradient of the domain size, which highlights the strong dependence of the domain size on Fe film thickness.

V. DISCUSSION

A. Orientation of domains

Except for very thin Fe film, below 3.3 ML, where the domains do not have well-defined stripe shape, the DWs in

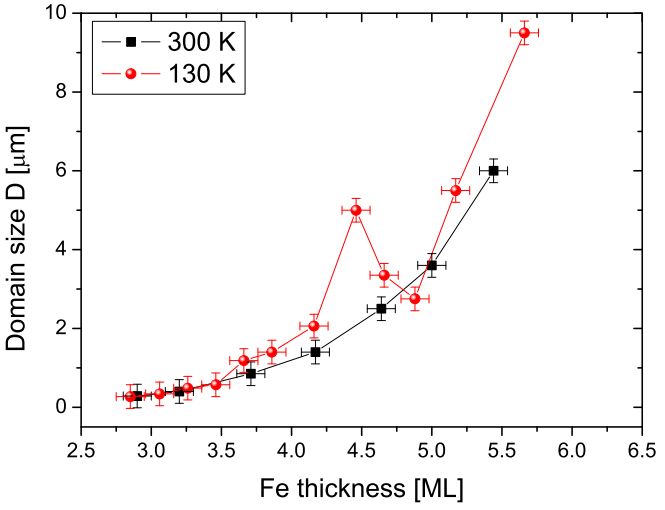

FIG. 4. Domain size D as a function of thickness of Fe film grown on a Ag(116) surface estimated from SPLEEM images obtained at 130 and 300 K. The size of domains is an averaged value over the area corresponding to the field of view (11.5 μm).

the canted state of magnetization are oriented perpendicular to the steps (see Fig. 1). This means that DWs lie along the $\varphi_{DW} = 90^\circ$ direction, which corresponds to the orientation of the tilted magnetization with the azimuthal angle $\varphi = 90^\circ$. It can be explained by the fact the nonparallel alignment of magnetization with respect to DWs is not energetically favorable, since the magnetostatic energy increases with the angle $\widetilde{\varphi} = \varphi - \varphi_{DW}$. Indeed, the magnetostatic energy (3), rewritten as

$$E_{dip}(t,D,\theta,\widetilde{\varphi}) = E_{dip}(t,D;\theta=0)\cos^2\theta + \left[2\pi M_s^2 - E_{dip}(t,D;\theta=0)\right]\sin^2\theta\sin^2\widetilde{\varphi}\,, \quad (12)$$

is clearly larger for nonzero $\widetilde{\varphi} \neq 0$ than for $\widetilde{\varphi} = 0$, since $2\pi M_s^2 > E_{dip}(t,D;\theta=0)$. The latter relation is satisfied because the magnetostatic energy of perpendicularly magnetized film ($\theta = 0$) becomes smaller after the stripe domains are formed; this can be proved in a strict way from Eq. (1), as shown in [28]. The fact that $E_{dip}(\theta,\widetilde{\varphi})$ is larger than $E_{dip}(\theta,\widetilde{\varphi}=0)$ can also be understood on more general grounds by using the expression $E_{dip} = \frac{1}{2}\int d\mathbf{r}\,\rho(\mathbf{r})\,\psi(\mathbf{r})$ [found from Eq. (A2) by partial integration], where for $\widetilde{\varphi} \neq 0$, the effective magnetic charge density $\rho(\mathbf{r}) = -\nabla_{\mathbf{r}}\psi$ has poles not only at the film surfaces, $\rho \sim \delta(z-0),\delta(z-t)$, but also on the domain walls, $\rho \sim \delta(x - nD)$ ($n = \ldots,-2,-1,0,1,2,\ldots$).

B. Evolution of the magnetization direction

The theory predicts that the transition from out-of-plane to in-plane orientation does not need to be accompanied by a vanishing effective anisotropy constant, responsible for decreasing domain size in films grown on atomically flat surfaces. Upon increasing the number of Fe layers N, the shape anisotropy (per unit film area) gradually increases and changes of the tilting angle can be briefly described in the following stages; $\theta = \alpha$ for $K_{dip}\sin 2\alpha = K_{sp}$, followed by $\theta = 45^\circ + \alpha$ for $K_{dip}\cos 2\alpha = K_s$ and eventually θ approaching 90° when K_{dip} dominates magnetocrystalline anisotropy terms K_s and K_{sp} for large N. Thus, the value of the tilting angle is governed by the interplay between the increasing shape anisotropy and two magnetocrystalline anisotropy terms, corresponding to two easy axes, (001) and (110), of the Fe film. Both differences $K_{dip}\cos 2\alpha - K_s$ and $K_{dip}\sin 2\alpha - K_{sp}$ that define the tilting angle in Eq. (11) also contribute to K_{eff} given by Eq. (10), but they do not vanish for the same film thickness. Therefore, the effective anisotropy K_{eff} within the plane perpendicular to the steps does not vanish during the SRT and, in fact, it can even increase upon increasing the film thickness, while magnetization rotates within this plane provided that K_s and K_{sp} have appropriate thickness dependencies.

The observed abrupt change of the magnetization direction from tilted, within the plane perpendicular to the steps to in-plane, parallel to the steps occurs at the thickness for which the energy

$$E_{||} = E(\theta = 90^\circ,\varphi = 0) = K_s - K_u \quad (13)$$

becomes lower than

$$E_{\perp,min} = E_\perp(\theta = \theta_0) = \tfrac{1}{2}(K_{dip} + K_s - K_{eff})\,. \quad (14)$$

These two expressions are obtained from Eqs. (7), (10), and (11), with $E_{bulk} = 0$. However, the condition $E_{||} < E_{\perp,min}$, written as

$$K_u > \tfrac{1}{2}(K_s - K_{dip} + K_{eff}), \quad (15)$$

does not gives a simple formula for the film thickness at which such discontinuous switching of magnetization orientation takes place.

C. Anisotropy constants

With the domain size D and the tilting angle $\theta = \theta_0$ measured experimentally with SPLEEM, the effective anisotropy constant K_{eff} can be found from Eqs. (2) and (5):

$$K_{eff} = A^{-1}\left[tM_s^2\ln(D/0.954t)\right]^2\cos^4\theta\,. \quad (16)$$

The obtained results for K_{eff} are shown in Fig. 5. The second relation between the anisotropy constants and the SPLEEM data is given by Eq. (11) for the tilting angle θ_0' from the terrace normal which corresponds to the tilting angle $\theta_0 = \theta_0' + \alpha$ from the film normal. In this way, we can determine from Eqs. (10) and (11) the two unknown magnetocrystalline anisotropy constants K_s and K_{sp}, since $K_{dip} = 2\pi M_s^2 t$ is known. They are given by the following formulas:

$$K_s = K_{dip}\cos 2\alpha + p_s K_{eff}|\cos 2\theta_0'|\,, \quad (17)$$

$$K_{sp} = K_{dip}\sin 2\alpha + p_{sp} K_{eff}|\sin 2\theta_0'|\,, \quad (18)$$

where, within the range $0^\circ \leqslant \theta_0 < 90^\circ$ of experimentally observed tilting angles, we have $p_s = 1$ for $\theta_0 \leqslant 45^\circ + \alpha$ and $p_s = -1$ for $\theta_0 > 45^\circ + \alpha$, while $p_{sp} = 1$ for $\theta_0 \leqslant \alpha$ and $p_{sp} = -1$ for $\theta_0 > \alpha$; the latter relations come from the energy minimum condition $\partial^2 E_\perp/\partial\theta^2 > 0$.

The obtained values of K_s, K_{sp} that reproduce the experimental values of the domain size and the tilting angle are shown in Fig. 5. Both anisotropy constants K_s and K_{sp} depend almost linearly on the Fe film thickness. A very similar linear dependence of K_s on the film thickness, with

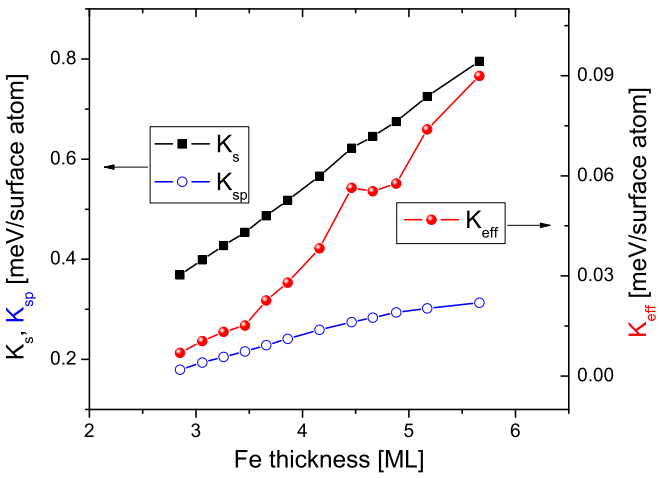

FIG. 5. Anisotropy constants K_{eff}, K_s, K_{sp} obtained from the tilting angle θ_0 and the domain size D measured in the SPLEEM experiment at $T = 130$ K. The values are obtained with the exchange stiffness constant $A = 1.49 \times 10^{-11}$ J/m.

K_s increasing from ~0.35 to ~0.70 meV (per surface atom) in the thickness range from 3 to 7 ML, was found experimentally for flat Fe/Ag(001) films [29]. The fact that the anisotropy constants K_s, K_{sp}, and K_{eff} are much larger than the fourth-order bulk anisotropy constant ($K_{bulk} = 5.4 \times 10^4 J/m^3$ [30], which corresponds to $0.0040 \times N$ meV/surface atom) justifies neglecting the bulk anisotropy term in our theoretical model for the investigated range of film thicknesses.

The canted structure in the vicinity of the SRT has been observed before for Ni [31,32] and Co [33] films grown on vicinal surfaces. In particular, it has been found that the canted magnetization is oriented within the plane perpendicular to the steps, which is predicted by our model to be a common characteristic of the SRT in ferromagnetic films on vicinal surfaces.

A local increase of the determined K_s, seen as a deviation from its roughly linear thickness dependence, is found at around 4.5 ML. The magnitude of this local oscillation as well as the resulting bump in the $K_{eff}(N)$ dependence are small. Nevertheless, this bump still leads to the significant increase of the domain size observed at ~ 4.5 ML, since D depends exponentially on the square root of the effective anisotropy constant. This clearly demonstrates that even small changes of surface anisotropy have a substantial effect on the domain structure. The local change in the domain size D at around 4.5 ML occurs solely at low temperature and therefore suggests to be related to quantum well states' (QWS) contribution to the magnetic anisotropy (which can be visible only at low temperature and only at specific thicknesses) [34,35]. Such a relation is strongly supported by the observation of large anisotropy of the orbital magnetic moment at this thickness, ascribed to the QWS from the d band (see Supplemental Material in [16]).

VI. SUMMARY AND CONCLUSIONS

In summary, we present a comprehensive study of the domain structure of Fe films grown on the Ag(116) vicinal surface. We show that upon increasing the film thickness, the canted magnetization in stripe domains rotate towards the sample plane within the plane perpendicular to the steps and simultaneously, the domain size increases exponentially. This increase is explained by the fact that in the Fe/Ag(116) stepped films the effective uniaxial anisotropy increases while the magnetization rotates towards the in-plane direction. We also demonstrate that with approaching the in-plane orientation, abrupt switching of the magnetization from perpendicular to the steps to parallel to the steps is observed and accompanied by characteristic splitting of the stripe domains. Using the values of the domain size and the magnetization orientation obtained from the experiment and basing on the theoretical model developed in this work, we provide the dependencies of the anisotropy constants on Fe film thickness. Additional interesting aspects beyond the scope of this paper include properties of domain walls and quantum well effects on the domain structure. To address these problems, further studies focused on higher resolution and lower temperature measurements are required.

APPENDIX: MAGNETOSTATIC ENERGY OF FERROMAGNETIC FILM WITH STRIPE DOMAINS FOR ARBITRARY DIRECTION OF MAGNETIZATION

The total magnetostatic energy

$$E_{dip} = \frac{1}{2}\int d\mathbf{r}\int d\mathbf{r}'\left(\frac{\mathbf{M}(\mathbf{r})\cdot\mathbf{M}(\mathbf{r}')}{|\mathbf{r}-\mathbf{r}'|^3} - \frac{3[\mathbf{M}(\mathbf{r})\cdot(\mathbf{r}-\mathbf{r}')][\mathbf{M}(\mathbf{r}')\cdot(\mathbf{r}-\mathbf{r}')]}{|\mathbf{r}-\mathbf{r}'|^5}\right) \quad \text{(A1)}$$

of a ferromagnetic system with continuous distribution of magnetization $\mathbf{M}$ can be represented as [36]

$$E_{dip} = \frac{1}{2}\int d\mathbf{r}\ \mathbf{M}(\mathbf{r})\cdot\nabla_{\mathbf{r}}\ \psi(\mathbf{r}) \quad \text{(A2)}$$

in terms of the scalar magnetic potential

$$\psi(\mathbf{r}) = \int d\mathbf{r}'\ \frac{\mathbf{M}(\mathbf{r}')\cdot(\mathbf{r}-\mathbf{r}')}{|\mathbf{r}-\mathbf{r}'|^3}\ . \quad \text{(A3)}$$

Let us note that, in fact, Eq. (A2) is the general formula for the potential magnetic energy, since $\mathbf{H} = -\nabla_{\mathbf{r}}\ \psi(\mathbf{r})$ is the static magnetic field produced by the ferromagnet.

For a film with stripe domains, the magnetization vector

$$\begin{aligned}\mathbf{M}(\mathbf{r}) &= [M_x(y), M_y(y), M_z(y)] \\ &= M(y)(\sin\theta\cos\widetilde{\varphi},\ \sin\theta\sin\widetilde{\varphi},\ \cos\theta)\end{aligned} \quad \text{(A4)}$$

varies along the y axis perpendicular to the DWs and does not depend on x and z, where the x axis is parallel to DWs and the z axis is perpendicular to the film surface. The periodic function $M(y)$ is defined as

$$M(y) = \begin{cases} -M_s & \text{for } -D + 2nD < y < 0 + 2nD \\ M_s & \text{for } 0 + 2nD < y < D + 2nD, \end{cases} \quad \text{(A5)}$$

where $n = \ldots, -1, 0, 1, \ldots$.

Then, the magnetostatic energy per unit volume, for the stripe domain system, is defined by

$$E_{dip} = \frac{1}{2}\frac{1}{(2D)t}\int_{-D}^{D} dy \int_0^t dz\ \mathbf{M}(\mathbf{r})\cdot\nabla_{\mathbf{r}}\ \psi(\mathbf{r}), \quad \text{(A6)}$$

since the magnetization $\mathbf{M}(x,y,z)$ does not depend on x and, consequently, the magnetic potential $\psi(x,y,z)$ is also independent of x. The latter conclusion immediately results from Eq. (A3) upon the substitution $x' \to x' + x$, which leads to the following expression for the magnetic potential:

$$\psi(\mathbf{r}) = \int d\mathbf{r}'\ \frac{M_y(y')(y-y') + M_z(y')(z-z')}{[(x')^2 + (y-y')^2 + (z-z')^2]^{3/2}} = -\int d\mathbf{r}'\left[M_y(y')\frac{\partial g(\mathbf{r},\mathbf{r}')}{\partial y} + M_z(y')\frac{\partial g(\mathbf{r},\mathbf{r}')}{\partial z}\right], \quad \text{(A7)}$$

where

$$g(\mathbf{r},\mathbf{r}') = [(x')^2 + (y-y')^2 + (z-z')^2]^{-1/2} = 1/|\mathbf{r}^* - \mathbf{r}'| \quad \text{(A8)}$$

is defined with $\mathbf{r}^* = (0, y, z)$. Then, from Eqs. (A6) and (A7), we find

$$E_{\rm dip} = -\frac{1}{4Dt}\int_{-D}^{D} dy \int_0^t dz \int d\mathbf{r}' \times \left[M_y(y)M_y(y')\frac{\partial^2 g}{\partial y'^2} + M_z(y)M_z(y')\frac{\partial^2 g}{\partial z'^2}\right] - \frac{3}{4Dt}\int_{-D}^{D} dy \int_0^t dz \int d\mathbf{r}' \times \frac{[M_y(y)M_z(y') + M_z(y)M_y(y')](y-y')(z-z')}{[(x')^2 + (y-y')^2 + (z-z')^2]^{5/2}}, \tag{A9}$$

where the relations $\partial^2 g/\partial y^2 = \partial^2 g/\partial y'^2, \partial^2 g/\partial z^2 = \partial^2 g/\partial z'^2$ have been used. The second term of $E_{\rm dip}$ in Eq. (A9) vanishes, since the substitution $z \leftrightarrow z'$ leads to the negative of this term. Also, one can add $M_y(y)M_y(y')\partial^2 g(\mathbf{r},\mathbf{r}')/\partial x'^2$ inside the brackets in the first term of $E_{\rm dip}$ in Eq. (A9) since the integral of $\partial^2 g(\mathbf{r},\mathbf{r}')/\partial x'^2$ over x' (within the limits $-\infty$ and ∞) vanishes. As a result, the magnetostatic energy is expressed as follows:

$$E_{\rm dip} = -\frac{1}{4Dt}\int_{-D}^{D} dy \int_0^t dz \int d\mathbf{r}' \left[M_y(y)M_y(y') \times \left(\frac{\partial^2 g}{\partial x'^2} + \frac{\partial^2 g}{\partial y'^2}\right) + M_z(y)M_z(y')\frac{\partial g}{\partial z'^2}\right]. \tag{A10}$$

Since the function $g(\mathbf{r},\mathbf{r}')$ satisfies the Poisson equation

$$\left(\frac{\partial^2}{\partial x'^2} + \frac{\partial^2}{\partial y'^2} + \frac{\partial^2}{\partial z'^2}\right) g(\mathbf{r},\mathbf{r}') = -4\pi\delta(\mathbf{r}' - \mathbf{r}^*), \tag{A11}$$

the above expression (A10) for $E_{\rm dip}$ can be further simplified to the following form:

$$E_{\rm dip} = \frac{\pi}{Dt}\int_{-D}^{D} dy \int_0^t dz M_y^2(y) - \frac{1}{4Dt}\int_{-D}^{D} dy \int_0^t dz \int d\mathbf{r}' \times [M_z(y)M_z(y') - M_y(y)M_y(y')]\frac{\partial^2 g}{\partial z'^2}. \tag{A12}$$

The calculation of the first integral in Eq. (A12) is straightforward since $M_y^2(y) = M_s^2 \sin^2\theta \sin^2\widetilde{\varphi}$ is constant throughout the film; see Eqs. (A4) and (A5). Thus, using the angle dependence of M_y and M_z, given in Eq. (A4), we get the following formula for the magnetostatic energy for arbitrary orientation of magnetization:

$$E_{\rm dip}(t,D,\theta,\widetilde{\varphi}) = 2\pi M_s^2 \sin^2\theta \sin^2\widetilde{\varphi} + (\cos^2\theta - \sin^2\theta \sin^2\widetilde{\varphi}) J(t,D) \tag{A13}$$

where

$$J(t,D) = -\frac{1}{4Dt}\int_{-D}^{D} dy \int_0^t dz \int d\mathbf{r}' \, M(y)M(y')\frac{\partial^2 g}{\partial z'^2}. \tag{A14}$$

From this relation we immediately see that

$$J(t,D) = E_{\rm dip}(t,D;\theta = 0) \tag{A15}$$

and, consequently, the final expression (3) for $E_{\rm dip}(t,D,\theta,\widetilde{\varphi})$ is obtained.

[1] Y. Yafet and E. M. Gyorgy, Phys. Rev. B **38**, 9145 (1988).
[2] B. Kaplan and G. Gehring, J. Magn. Magn. Mater. **128**, 111 (1993).
[3] B. Kaplan, J. Magn. Magn. Mater. **298**, 135 (2006).
[4] O. Portmann, A. Vaterlaus, and D. Pescia, Nature (London) **422**, 701 (2003).
[5] K. Man, M. Altman, and H. Poppa, Surf. Sci. **480**, 163 (2001).
[6] H. P. Oepen, M. Speckmann, Y. Millev, and J. Kirschner, Phys. Rev. B **55**, 2752 (1997).
[7] H. P. Oepen, Y. T. Millev, and J. Kirschner, J. Appl. Phys. **81**, 5044 (1997).
[8] M. Speckmann, H. P. Oepen, and H. Ibach, Phys. Rev. Lett. **75**, 2035 (1995).
[9] Y. Z. Wu, C. Won, H. W. Zhao, and Z. Q. Qiu, Phys. Rev. B **67**, 094409 (2003).
[10] D. Stickler, R. Frömter, H. Stillrich, C. Menk, H. P. Oepen, C. Gutt, S. Streit-Nierobisch, L.-M. Stadler, G. Grübel, C. Tieg *et al.*, Phys. Rev. B **84**, 104412 (2011).
[11] E. Bauer, T. Duden, H. Pinkvos, H. Poppa, and K. Wurm, J. Magn. Magn. Mater. **156**, 1 (1996).
[12] D. E. Bürgler, C. M. Schmidt, D. M. Schaller, F. Meisinger, R. Hofer, and H.-J. Güntherodt, Phys. Rev. B **56**, 4149 (1997).
[13] R. K. Kawakami, E. J. Escorcia-Aparicio, and Z. Q. Qiu, Phys. Rev. Lett. **77**, 2570 (1996).
[14] Y. Z. Wu, C. Won, and Z. Q. Qiu, Phys. Rev. B **65**, 184419 (2002).
[15] U. Bauer and M. Przybylski, Phys. Rev. B **81**, 134428 (2010).
[16] M. Dąbrowski, T. Peixoto, M. Pazgan, A. Winkelmann, M. Cinal, T. Nakagawa, Y. Takagi, T. Yokoyama, F. Bisio, U. Bauer, *et al.*, Phys. Rev. Lett. **113**, 067203 (2014).
[17] C. Kooy and U. Enz, Philips Res. Rep. **15**, 7 (1960).
[18] K. Grzelakowski and E. Bauer, Rev. Sci. Instrum. **67**, 742 (1996).
[19] N. Rougemaillea and A. K. Schmid, Eur. Phys. J. Appl. Phys. **50**, 20101 (2010).
[20] E. Bauer, T. Duden, and R. Zdyb, J. Phys. D **35**, 2327 (2002).
[21] J. Maxson, N. Perkins, D. Savage, A. Woll, L. Zhang, T. Kuech, and M. Lagally, Surf. Sci. **464**, 217 (2000).
[22] M. S. Altman, J. Phys.: Condens. Matter **22**, 084017 (2010).
[23] M. Stampanoni, A. Vaterlaus, M. Aeschlimann, and F. Meier, Phys. Rev. Lett. **59**, 2483 (1987).
[24] Z. Q. Qiu, J. Pearson, and S. D. Bader, Phys. Rev. B **49**, 8797 (1994).
[25] R. Allenspach, M. Stampanoni, and A. Bischof, Phys. Rev. Lett. **65**, 3344 (1990).
[26] R. Zdyb, A. Locatelli, S. Heun, S. Cherifi, R. Belkhou, and E. Bauer, Surf. Interface Anal. **37**, 239 (2005).

[27] R. Ramchal, A. K. Schmid, M. Farle, and H. Poppa, Phys. Rev. B **68**, 054418 (2003).
[28] A. B. Kashuba and V. L. Pokrovsky, Phys. Rev. B **48**, 10335 (1993).
[29] R. J. Hicken, S. J. Gray, A. Ercole, C. Daboo, D. J. Freeland, E. Gu, E. Ahmad, and J. A. C. Bland, Phys. Rev. B **55**, 5898 (1997).
[30] S. Bodea, W. Wulfhekel, and J. Kirschner, Phys. Rev. B **72**, 100403 (2005).
[31] C. Klein, R. Ramchal, A. K. Schmid, and M. Farle, Phys. Rev. B **75**, 193405 (2007).
[32] S. S. Dhesi, H. A. Dürr, and G. van der Laan, Phys. Rev. B **59**, 8408 (1999).
[33] A. Stupakiewicz, A. Maziewski, K. Matlak, N. Spiridis, M. Slezak, T. Slezak, M. Zajac, and J. Korecki, Phys. Rev. Lett. **101**, 217202 (2008).
[34] J. Li, M. Przybylski, F. Yildiz, X. D. Ma, and Y. Z. Wu, Phys. Rev. Lett. **102**, 207206 (2009).
[35] M. Przybylski, M. Dąbrowski, U. Bauer, M. Cinal, and J. Kirschner, J. Appl. Phys. **111**, 07C102 (2012).
[36] J. D. Jackson, *Classical Electrodynamics* (John Wiley & Sons, Ltd., New York, 1998).